Towards Reducing the Cost of Key Components in PEM Fuel Cells: Optimizing Platinum Catalyst Loading and Enhancing Technology Robustness

J. Isidro*, L. Sánchez-Beato, I. Ayuso, J. Rodríguez and R. Campana

Spanish National Hydrogen and Fuel Cell Technology Testing Centre, Prolongación Fernando el Santo, s/n. 13500 Puertollano, Ciudad Real, Spain

*Corresponding author: julia.isidro@cnh2.es

Paper enrolled on the XXVI Meeting of the Portuguese Electrochemical Society

Received 02/04/2026; accepted 02/05/2026
https://doi.org/10.4152/pea.2027450520

Abstract

In this work, the electrochemical performance of various Membrane Electrode Assemblies (MEAs) using Nafion® membranes (NR211, XL, NR212 and N115) incorporating low platinum-loading electrodes (0.05 and 0.1 mg_{Pt} cm^{-2}), developed with two different commercial catalyst 60% Pt/C and 40% Pt/C, have been evaluated. The electrodes were manufactured depositing the catalytic ink, prepared with catalyst HiSPEC4000 and HiSPEC9100, onto the gas diffusion layers, by wet powder spraying. In order to carrying out this study, a robust testing protocol for Proton Exchange Membrane Fuel Cells (PEMFCs) was designed, consisting of three steps: activation, polarization curve measurements (current-voltage), and Electrochemical Impedance Spectroscopy (EIS). Tests were repeated to assess the effects of oxidant (air or oxygen) and operating pressure, with parameters adjusted sequentially: air atmospheric → air + 1 bar → air + 2 bar → O2 atmospheric → O2 + 1 bar → O2 + 2 bar. Results point out that, by the increasing of the back pressure consistently, the maximum power density across all four MEAs is improved, regardless of oxidant. Switching from air to oxygen led to significant power increases of 57.3, 56.6, 54.3, and 37.2% for MEAs with Nafion® NR211, XL, NR212, and N115, respectively. This suggests that thicker membranes result in higher PEMFCs performance due to lower internal resistance. The MEA with Nafion® NR211 (25 μm thickness) achieved the highest performance, emphasizing that reducing membrane thickness enhances functionality. This insight will inform future research on optimizing membrane thickness. Additionally, reducing platinum content in the catalyst from 60 to 40% Pt/C in NR211 and NR212 membranes showed stable performance, confirming their suitability with lower Pt concentrations. The new catalyst formulation performed better than the previous one under H_2/O_2 and higher back pressures, where lower Pt loading limitations become more apparent.

Keywords: low Pt load; PEM fuel cell; Nafion® membranes; test protocol.

Graphical Abstract

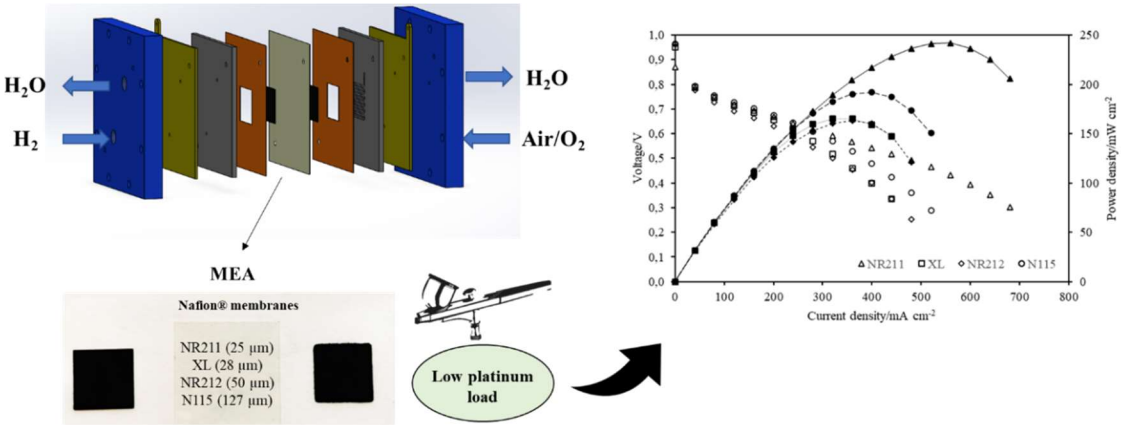

Introduction•

Energy management has become a critical global issue due to the increasing demand for sustainable and efficient energy sources. The depletion of fossil fuels, environmental concerns, and climate change have driven the search for cleaner alternatives. Renewable energy sources such as solar, wind, and hydropower have gained significant attention; however, their intermittent nature poses a challenge for stable energy supply [1, 2]. Hydrogen, particularly green hydrogen, has emerged as a promising solution due to its potential for clean energy production and storage [3]. Among the various hydrogen-based technologies, Proton Exchange Membrane Fuel Cells (PEMFCs) have gained prominence due to their efficiency and applicability in transportation, stationary, and portable power generation [4].

The global reliance on fossil fuels has led to environmental degradation, including greenhouse gas emissions and air pollution. As a result, there is an urgent need for alternative energy solutions that are sustainable, efficient, and environmentally friendly. Renewable energy technologies have shown potential, but they require effective energy storage and conversion methods to ensure reliability [5]. Hydrogen-based energy systems have gained interest because hydrogen is an abundant element and can be produced using various methods, including electrolysis powered by renewable sources. When used in fuel cells, hydrogen can generate electricity efficiently while producing only water as a by-product, making it a clean energy carrier.

Green hydrogen, produced through water electrolysis using renewable energy, is considered a key component in the future of sustainable energy. Unlike grey or blue hydrogen, which are derived from fossil fuels, green hydrogen does not contribute to carbon emissions. The widespread adoption of green hydrogen can help mitigate climate change by reducing dependency on conventional energy

•The abbreviations list is in pages 673-74.

sources. However, several challenges remain, including production costs, infrastructure development, and energy conversion efficiency. Fuel cells, particularly PEMFC, offer a viable solution for utilizing hydrogen efficiently and sustainably [6, 7].

PEMFC are widely recognized for their high efficiency, low operating temperatures, and fast start-up capabilities. They consist of an anode, a cathode, and a proton-conducting membrane. Hydrogen is fed into the anode, where it undergoes oxidation, releasing protons and electrons. The protons travel through the membrane to the cathode, while the electrons flow through an external circuit, generating electricity. At the cathode, the protons and electrons combine with oxygen to produce water. This reaction provides a clean and efficient energy conversion process suitable for various applications, including electric vehicles, stationary power systems, and portable devices.

The performance of PEMFC is highly dependent on the type of membrane used, as it directly affects proton conductivity, mechanical stability, and durability. Nafion® membranes are the most widely used due to their excellent proton conductivity and chemical stability. Normally, Nafion® 117 has been widely used over the years due to its stability and its ability to operate at temperatures above 80 °C, not only in fuel cells but also in electrolysis [8]. However, there are other types of Nafion® membranes characterized by lower thickness that need to be further investigated to optimize fuel cell performance, such as NR211, XL, NR212, and N115 [9-11]. Each membrane type has distinct properties that influence water retention, mechanical strength, and fuel crossover. Research efforts focus on improving the durability and efficiency of these membranes to enhance the overall performance of PEMFC.

The catalytic layer of PEMFC plays a crucial role in the electrochemical reactions occurring at the electrodes. Platinum-based catalysts are the most commonly used due to their high catalytic activity and stability. The typical platinum catalytic loading in PEMFC ranges from 0.1 to 0.5 mgPt cm^{-2} [12-14]. However, platinum is a rare and expensive metal, posing challenges for large-scale commercialization. To address this issue, research has focused on reducing platinum loading while maintaining fuel cell efficiency. Recent studies have explored low platinum loadings to optimize cost and performance [15]. Additionally, alternative catalyst materials, such as platinum alloys and non-precious metal catalysts, are being investigated to further reduce reliance on platinum.

The management of energy resources is a pressing challenge that requires innovative solutions for sustainable and efficient power generation. Green hydrogen and PEMFC present promising alternatives to conventional fossil fuels, offering clean and efficient energy conversion. Advances in membrane technology, such as different Nafion membranes, and optimized platinum catalyst loading strategies are crucial for improving fuel cell performance and economic feasibility. Continued research and development in these areas will drive the

widespread adoption of hydrogen-based energy systems, paving the way for a cleaner and more sustainable future.

Taking into account the arguments previously described, this work aims, in an early stage, to identify which membranes exhibit higher performance in terms of power density by conducting an in-depth comparative study of different types of polymeric membranes used in PEMFC. In a later stage, the impact of reducing the platinum content of the catalyst for the electrode fabrication of these systems will be studied.

Materials and methods

Catalytic inks were prepared by dispersing a fixed amount of catalyst (platinum supported on carbon nanoparticles, Pt/C powder) in a Nafion® solution (Aldrich, 5 wt%, in low molecular weight aliphatic alcohols) and ethanol (VWR Chemicals, 96% v/v) using an ultrasonic bath. The commercial catalysts used contained 40 wt% and 60 wt% Pt/C (HiSPEC4000 and HiSPEC9100, respectively). Electrode fabrication was performed by spraying the electrocatalytic ink onto the microporous face of the gas diffusion layer (GDL, Freudenberg Group H23C2) with an airbrush (VEGA 2000). The resulting electrodes had catalytic loadings of 0.05 mgPt cm^{-2} and 0.1 mgPt cm^{-2}.

Membrane electrode assemblies (MEAs) were directly assembled within a Scribner single cell with a 5 cm^2 active area. Nafion® membranes of varying thicknesses, including NR211 (25 µm, QuimTech), XL (28 µm, Fuel Cell Store), NR212 (50 µm, Ion Power), and N115 (127 µm, Thermo Fisher Scientific) were positioned between the electrodes, with a clamping torque of 2 Nm applied.

The *in situ* electrochemical characterizations of the MEAs was performed using a Scribner 850e Fuel Test System under the following experimental conditions: cell and gas temperatures were maintained at 70 °C, with a relative humidity of 100% for both gases. Reactant gases were supplied at atm pressure, +1 bar, and +2 bar back pressures, with flow rates of 0.05 L min^{-1} for hydrogen (anode) and 0.1 L min^{-1} for air or oxygen (cathode), respectively.

Electrochemical testing proceeded as follows: initially, MEAs were operated under a constant current density of 200 mA cm^{-2} until a steady-state voltage was reached. Subsequently, polarization curves (I-V curves) were recorded, followed by electrochemical impedance spectroscopy (EIS) measurements. EIS was conducted using a potentiostat-galvanostat (AUTOLAB PGSTAT302N), applying a sinusoidal current signal with an amplitude of 100 mA at 1 A across a frequency range from 0.1 Hz to 100 kHz. Impedance spectra were analysed and fitted using the EIS Spectrum Analyzer software.

The *ex-situ* microstructural characterization of the electrode surfaces and MEAs cross-sections was conducted using scanning electron microscopy (SEM, JEOL 6010PLUS/LA) at an acceleration voltage of 15 kV in secondary electron and backscattered electron modes + Energy Dispersive Spectroscopy module. MEAs cross-sections were prepared by embedding each sample in a binary resin mould

and curing it for 24 h. The encapsulated MEAs were then sectioned, polished, and gold-coated to enhance conductivity and ensure high-resolution imaging during SEM analysis. The characterization of the electrodes surfaces for each type of electrode used in this study is shown in Fig. 1, where it can be observed that for both catalysts used (60 wt% and 40 wt% Pt/C), the electrodes with a lower catalytic loading (0.05 mg Pt cm^{-2}) exhibit a lower platinum concentration. The electrodes with less catalytic load also show a lower surface platinum content. However, in the case of electrodes fabricated with the catalyst containing a lower platinum concentration (40 wt% Pt/C), an even lower amount of platinum is observed on the surface. This may be related to the deposition of a greater number of catalytic layers.

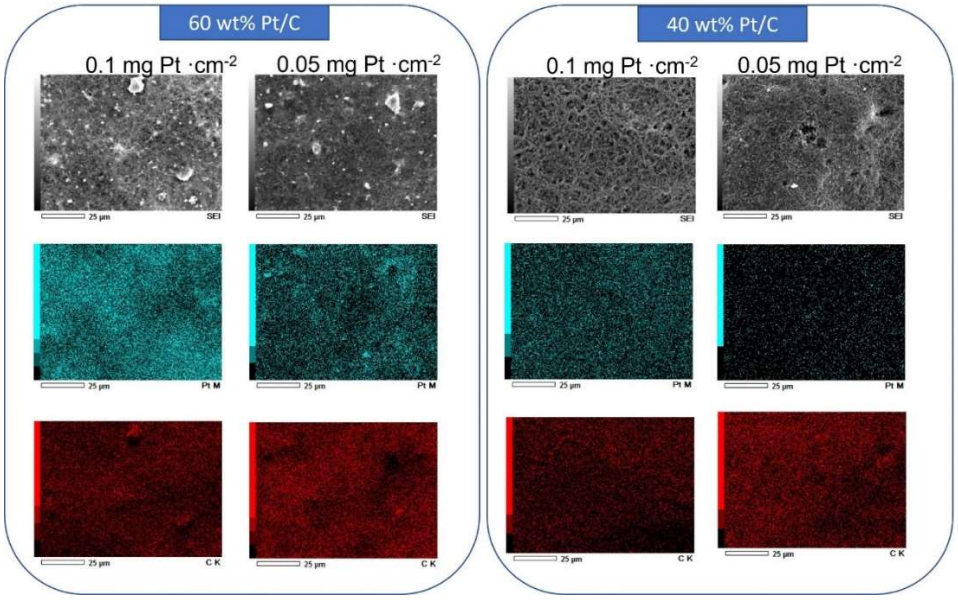

Figure 1: SEM images of the electrodes prior to be assembled to conform the MEAs (upper part); EDS analysis of the platinum and carbon distribution for each type of electrode produced to carried out this work.

Results and discussion

Comparative study of the performance of different Nafion® membranes

MEAs analysed in the study were fabricated using a fixed amount of catalyst (60% Pt/C, HISPEC 9100) and Nafion® solution as a binder, but incorporated different Nafion® membranes. The catalytic layers were prepared with varying platinum loadings: 0.1 mg Pt cm^{-2} on the cathode and 0.05 mg Pt cm^{-2} on the anode, resulting in a total platinum loading of 0.15 mg Pt cm^{-2}.

Membrane electrode assemblies' activation at constant current

Prior to electrochemical characterization, the MEAs underwent a 20 h. conditioning process. This electrical conditioning was performed in single cells at a constant current density of 200 mA cm^{-2}. Fig. 2 presents the voltage variation of the single cells recorded during this conditioning phase.

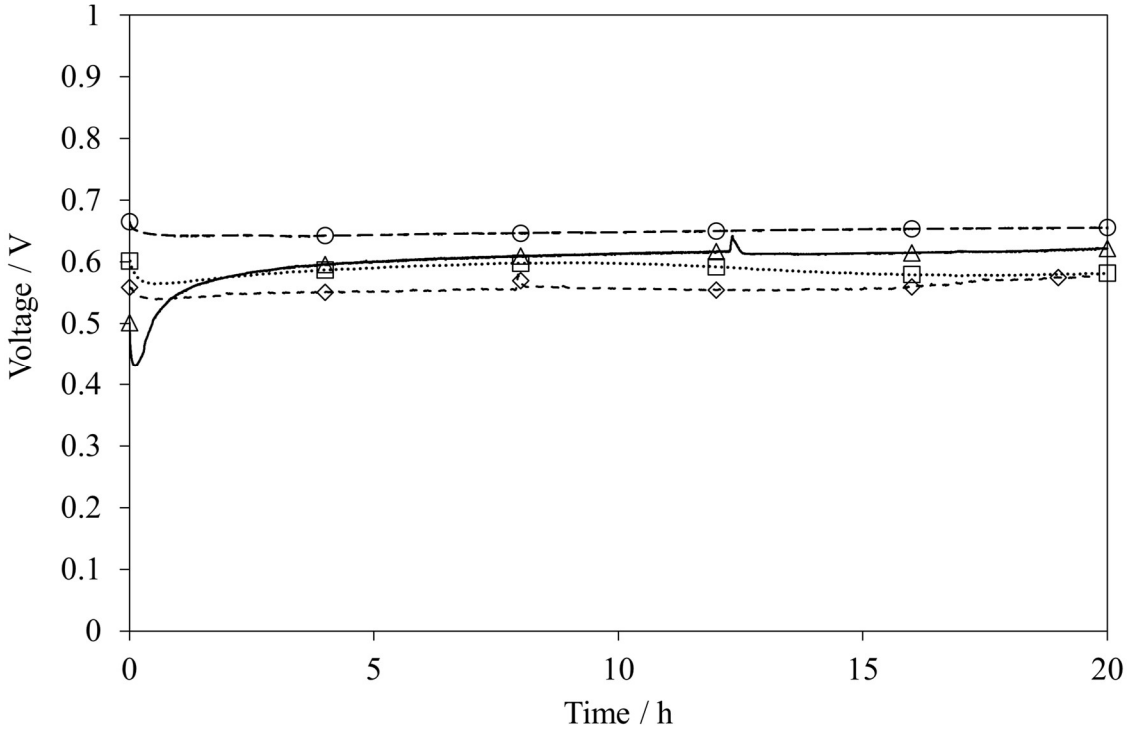

Figure 2: Voltage-time curves of MEAs tested at a current density of 0.2 A cm^{-2}, with H_2/air supplied at atmospheric pressure during 20 ~~hrs~~. The symbols represent different Nafion®membranes: △ NR211; □ XL; ◇ NR212; ○ N115.

The cells exhibited transient voltages behaviour until a steady state was achieved. During activation phase of MEAs at a current density of 200 mA cm^{-2}, final voltage values varied depending on the membrane used. The lowest final voltage was observed for the MEA with Nafion® NR212 (0.576 V). In contrast, MEAs incorporating membranes of different thicknesses ― Nafion® NR211, XL and N115― achieved higher final voltages of 0.622, 0.584 and 0.656 V, respectively. Among these, the MEA utilizing Nafion® N115 displayed the highest final voltage, indicating superior performance during the activation phase [16, 17]. Upon completion of the conditioning and electrical activation processes, the MEAs underwent electrochemical characterization consisting of polarization curves and Electrochemical Impedance Spectroscopy measurements (EIS) under the different conditions studied.

Polarization curves

The electrochemical performance of the MEAs was evaluated through polarization curves and electrochemical impedance spectra obtained for each single cell. Fig. 3 presents polarization curves of MEAs using H_2/Air (a, b, c) and H_2/O_2 (d, e, f) as reactant gases at atm. pressure (P_{atm}) (a, d), +1 bar (b, e), and +2 bar (c, f) back pressure. The remaining operating parameters-including cell and reactant gas temperatures and flow rates and relative humidity-were kept constant, as described in the Materials and Methods section.

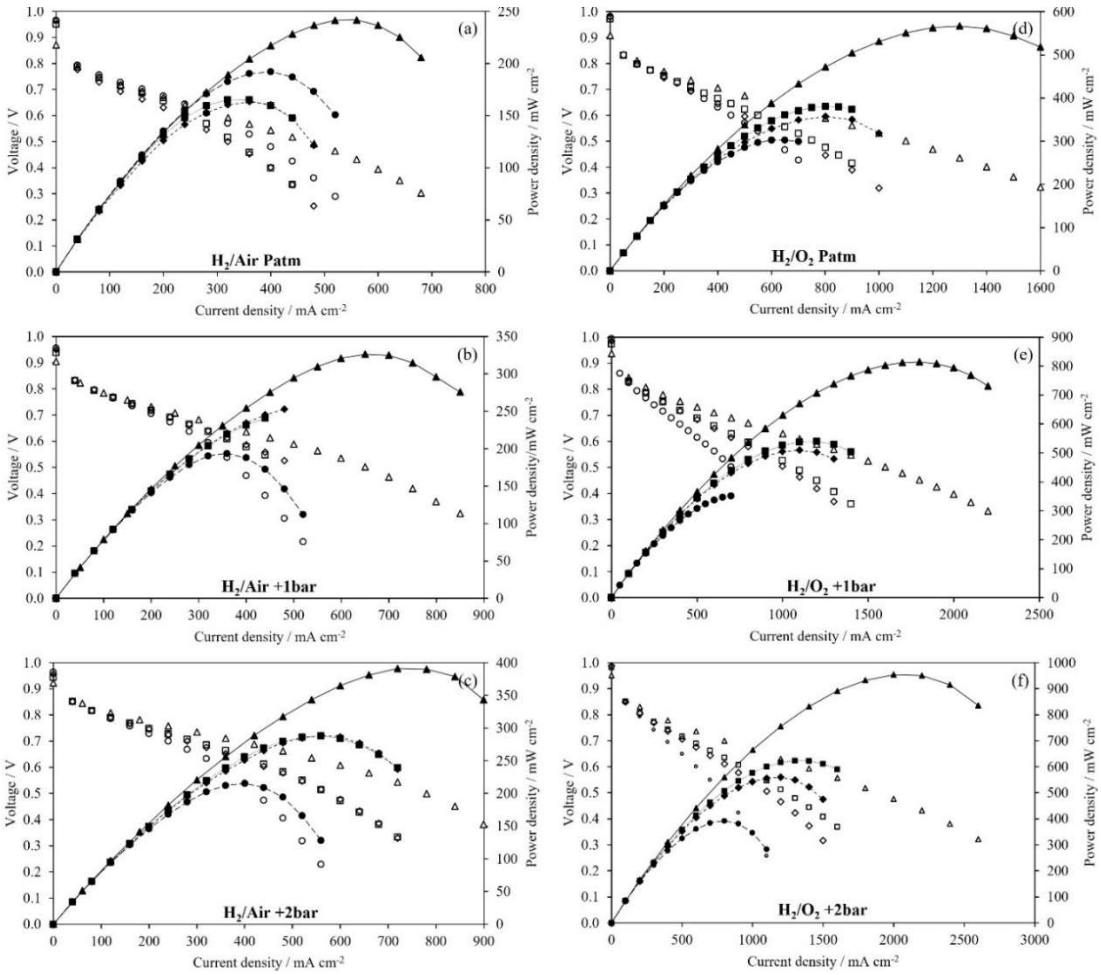

Figure 3: Current density-voltage (I-V) and current density-power density (I-P) curves of MEAs with different Nafion® membranes: △ NR211, □ XL, ◇ NR212, and ○ N115.

From the analysis of the polarization curves, open-circuit voltages (OCV), maximum power densities (P_{max}), and Pt-specific power parameter (Pt_{TC}) for the tested MEAs are summarized in Table 1.

Table 1: OCV, P_{max}, and Pt_{TC} at P_{max} evaluated for the tested MEAs under different gas compositions and operating pressures.

Naflon®	**OCV (V)** **Pmax (mW cm^{-2})** **Pt_{TC} (g_{Pt} kW^{-1})**	**H_2/Air Pambient**	**H_2/Air +1bar**	**H_2/Air +2bar**	**H_2/O_2 Pambient**	**H_2/O_2 +1bar**	**H_2/O_2 +2bar**
NR211	OCV	0.871	0.905	0.922	0.909	0.937	0.951
	Pmax	242	326	391	567	814	954
	Pt_{TC}	0.630	0.467	0.390	0.269	0.187	0.160
XL	OCV	0.950	0.938	0.943	0.972	0.974	0.981
	Pmax	165	246	288	380	540	623
	Pt_{TC}	0.936	0.628	0.537	0.406	0.286	0.248
NR212	OCV	0.966	0.950	0.956	0.980	0.984	0.987
	Pmax	163	254	288	357	510	559
	Pt_{TC}	0.987	0.635	0.559	0.451	0.316	0.288
N115	OCV	0.966	0.955	0.964	0.981	0.994	1.005
	Pmax	190	194	215	303	352	392
	Pt_{TC}	0.801	0.787	0.707	0.503	0.433	0.388

The Pt_{TC} parameter was calculated according the Eq. (1):

$$Pt_{TC} = \frac{L_{Pt}}{P_{max}} \quad (1)$$

where L_{Pt} is the Pt loading (g_{Pt} cm^{-2}) and the P_{max} is the maximum power density output (kW cm^{-2}).

As shown in Fig. 3, it becomes evident that operating parameters such as backpressure [18] and the oxidizing gas used (air or oxygen) have a significant influence on the electrochemical performance of the studied MEAs, affecting the OCV, electrode kinetics, and mass transport processes, and, to a lesser extent, the electrolyte resistance. Additionally, other factors such as the Nafion® content in the catalytic layer, the thickness of these layers, and the membrane thickness also influences performance. The combined impact of these variables on cell performance was evaluated using two key metrics: maximum electrical power density and mass platinum per unit power (Pt_{TC}), which will be further discussed in the following sections.

Maximum power density for the Nafion® membranes studied

To discuss the results of this section, it is important to consider several Key Performance Indicators (KPIs) defined by the U.S. Department of Energy (DOE) and EU Harmonised Test Protocols for PEMFC MEA testing in automotive applications [4, 19], which stablish performance benchmarks, such as power density targets (mW cm^{-2}) and platinum group metal (PGM) content goals (gPGM kW^{-1}). Following these protocols, the testing procedure defined in the Materials and Methods section was stablished to study the effects of the supplied oxidant gas and the applied backpressure.

The polarization curves (Fig. 3) reveal a consistent trend for all tested MEAs: maximum power density increases with increasing operating pressure and when the oxidant is switched from air to pure oxygen at the same pressure. In particular, increasing the backpressure from atmospheric conditions to + 2bar consistently enhances the power density by approximately 60-70% for all tested membranes. In addition, the use of pure oxygen leads to a further improvement in the cell efficiency, especially at low pressures. These results confirm that backpressure and oxidant type are key factors governing MEAs performance, as higher pressure improves gas diffusion and reduces mass transport limitations, while oxygen enhances cathode reaction kinetics.

Another important aspect is the influence of the membrane properties on electrochemical performance, as evidenced in Fig 3 and Table 1. Thus, Nafion® NR211 (25 μm) exhibited the highest performance across most operating conditions, followed by Nafion® XL (27.5 μm), while Nafion® NR212 (50 μm) and N115 (127 μm) showed lower values. The thinner membrane, Nafion® NR211 achieved power densities above 900 mW cm^{-2} under H_2/O_2 owing to its lower ohmic resistance and higher proton conductivity, whereas the thicker membrane,

Nafion® N115, showed the lowest performance under H_2/air conditions but improves significantly under elevated pressure and oxygen-rich conditions, reaching values above 500 mW cm^{-2}.

At this point, it is important to note that Nafion® not is only use as a membrane but is also incorporated as a binder in the catalytic inks as it plays an important role on three concurrent processes occurring in the catalytic layer: (1) the accessibility of reactant gases to the catalytically active sites, which are partially covered by the ionomer, (2) proton conductivity through the ionomer, and (3) electron transport through the catalyst's carbonaceous support, which is partially impregnated with Nafion®, an electronic insulator. Together, these factors highlight the complex interplay of material properties and operating conditions in determining fuel cell efficiency. Nevertheless, this not affect the comparison of the experiments carried out in this work, since the Nafion® content in the catalytic ink, as well as the catalyst loading of the electrodes in all the studied MEAs, was kept constant.

The trends described previously are further confirmed in Fig. 4, which summarizes the maximum power densities obtained under the different operating conditions for each of the MEAs studied. Fig. 4b highlights important trends in the variation of peak power density (P_{max}) as influenced by Nafion® membrane thickness and different operating conditions. Thinner membranes, such as Nafion® NR211 (25 µm), consistently demonstrated the highest increases in P_{max}. This behaviour can be attributed to their lower ohmic resistance and enhanced proton conductivity, which are critical for optimizing performance in PEMFCs. In contrast, thicker membranes like Nafion® N115 (127 µm) exhibited smaller variations in P_{max}, reflecting their higher internal resistance and reduced efficiency in facilitating proton transport. The results of the analysis of these resistances using EIS will be presented and discussed in a s subsequent section.

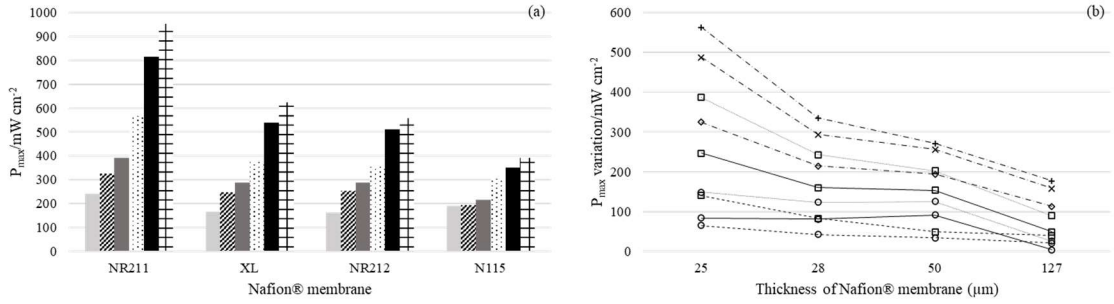

Figure 4: (a) Peak power densities of MEAs as a function of Nafion® membranes for different operating conditions- ■H_2/air and ⁘ H_2/O_2 at atm pressure, ▨ H_2/air and ■H_2/O_2 at +1 bar back pressure and ■H_2/air and # H_2/O_2 at +2 bar back pressure; **(b)** Variations in P_{max} as a function of Nafion® membranes thickness for H_2/air (○) and H_2/O_2 (□) at pressure differentials of +1 bar-atm, +2bar-atm, and +2bar-+1bar. Additionally, changes in P_{max} between H_2/O_2 and H_2-air are shown for atm pressure (◇), +1 bar back pressure (×), and +2 bar back pressure (+).

Overall, the results demonstrate that both operating conditions (oxidant type and operating pressure) and the intrinsic properties of the membrane are key factors determining the performance of MEAs for PEMFC. Additionally, the type of oxidizing gas had a notable impact. Increasing the pressure and using pure oxygen significantly enhance power density by promoting gas diffusion and reducing mass transport limitations, while the thinner membrane (such as Nafion® NR211) provide superior performance due to their lower ohmic resistance and higher proton conductivity. These findings highlight the interplay between operational conditions and the electrochemical behaviour of the tested MEAs, providing a robust foundation for further analysis.

Pt-specific power for the Nafion® membranes studied

This parameter represents the amount of Pt required to generate a unit of power. Therefore, lower Pt_{TC} indicate a more efficient platinum utilization, since less catalyst is needed to achieve the same power output. Consequently, values approaching zero correspond to a higher Pt utilization efficiency. This, Fig. 5 illustrates the correlation between this parameter (Pt_{TC}) and the type of Nafion® membrane across different operating conditions. As can be observed, Nafion® NR211 consistently achieved the lowest Pt_{TC} values, demonstrating superior catalytic efficiency. Notably, under high pressures and pure oxygen (H_2/O_2 at +2 bar back pressure), Pt_{TC} for NR211 dropped below 0.3 g_{Pt} kW^{-1}, indicating enhanced utilization of platinum. In contrast, thicker membranes, such as Nafion® N115, exhibited significantly higher Pt_{TC} values, exceeding 0.8 g_{Pt} kW^{-1} under atm pressure with H_2/air, reflecting poorer platinum efficiency.

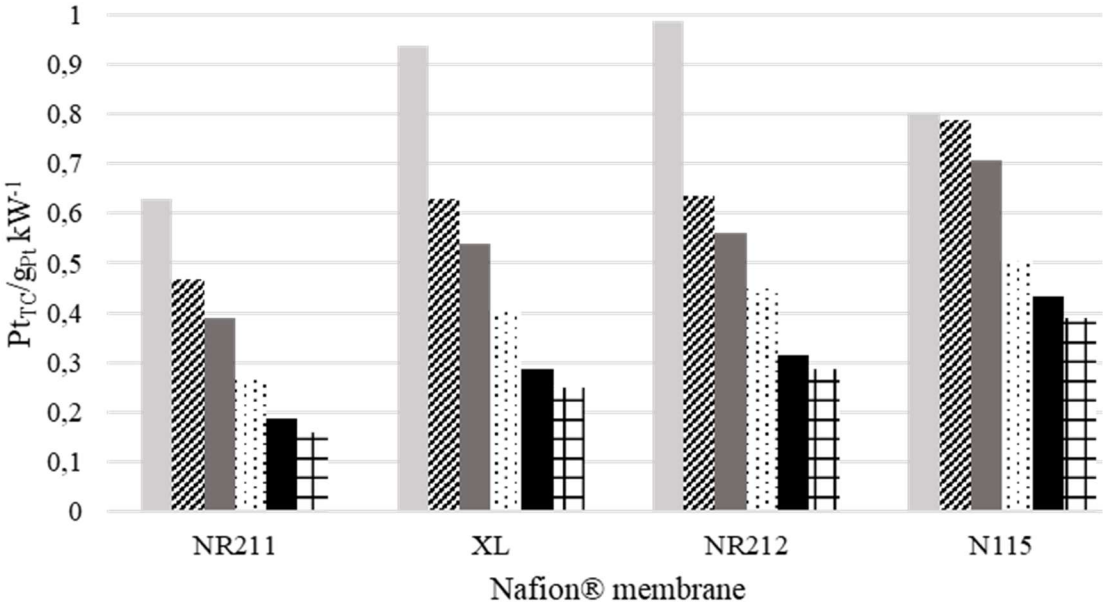

Figure 5: Platinum mass per kW (Pt_{TC}) versus Nafion® membranes at different gases configuration- ■H_2/air and ⁘ H_2/O_2 at atm pressure, ▨ H_2/air and ■H_2/O_2 at +1 bar back pressure and ■H_2/air and # H_2/O_2 at +2 bar back pressure.

The observed trends underscore the critical influence of membrane thickness and operational parameters on platinum utilization. Increased operating pressure and the use of pure oxygen consistently improved Pt_{TC} values across all membranes, attributed to enhanced cathodic reaction kinetics and reduced mass transport limitations. These findings again highlight the importance of optimizing membrane characteristics and operating conditions to achieve efficient catalytic performance in PEMFCs.

Electrochemical impedance spectroscopy (EIS)

Another important electrochemical parameter to be analyse is the electrochemical impedance spectra of MEAs, as it can be used to determine the different resistances present in this type of systems. In this case, EIS were measured in galvanostatic mode at a current of 1 A, using H_2/air and H_2/O_2 as reactant gases under atm conditions, 1 bar and 2 bar back pressure. Nyquist plots corresponding to these measurements are presented in Fig. 6 (a–f).

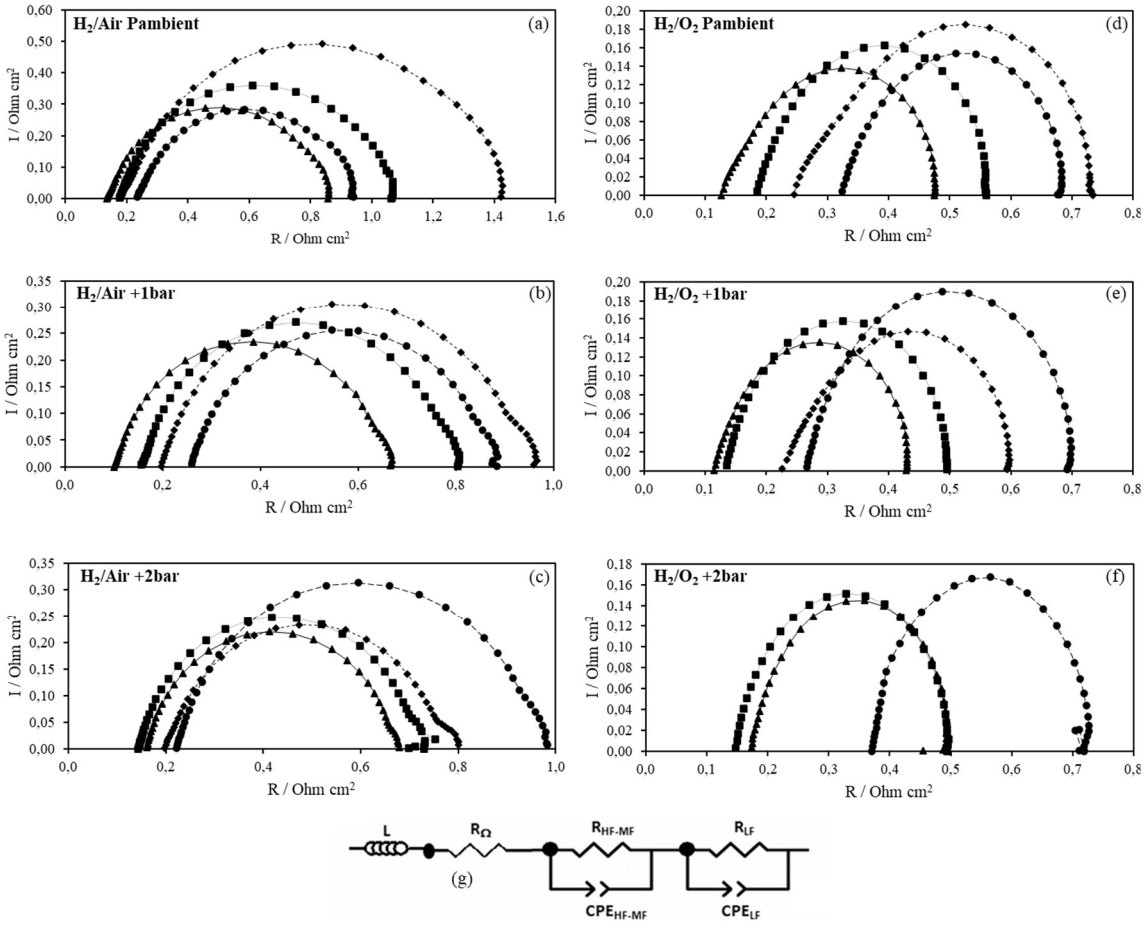

Figure 6: Nyquist diagrams (**a-f**) for MEAs incorporating different Nafion® membranes- △ NR211, □ XL, ◇ NR212, and ○ N115, tested under galvanostatic mode (1 A) across a frequency range from 0.1 Hz to 100 kHz, under various gas compositions and operating pressures. Additionally, **(g)** shows corresponding equivalent circuit used for fitting impedance data.

Ohmic (R_Ω) and total resistance (R_T) were determined from the high-and low-frequency intercepts of the impedance spectra with the real axis (Z_{Re}), respectively. Nyquist diagrams display depressed semicircles, typical of PEMFCs. MEAs employing Nafion® NR211 membrane (△) consistently exhibited the smallest high-frequency arcs, indicating minimal R_Ω.

This superior performance is attributed to its thin structure (25 μm), which enhances proton conductivity. Nafion® XL membrane (□) also showed good performance, but with slightly higher resistance. In contrast, thicker membranes such as Nafion® N115 (○) displayed the largest low frequencies, that could be attributed to mass transport limitations associated with it higher thickness and reduced gas diffusivity.–Nafion® NR212 membrane (◇) showed intermediate behaviour between NR211 and N115, in line with the expected performance based on membrane thickness.

The equivalent circuit used to fit the impedance spectra, shown in Fig. 6 g, includes a pseudo-inductance (L), associated with metallic components and current collectors, together with R_Ω and two parallel resistor constant-phase element (CPE) contributions connected in series.

Table 2 summarizes the estimated ohmic (R_Ω), polarization (R_P) and total (R_T) resistances values for the different Nafion®-based MEAs under varying gas compositions and pressure conditions.

Table 2: Estimated ohmic, polarization and total resistance of the studied MEAs under different gas and pressure operation modes.

Naflon®	Gas mode pressure	R_Ω (Ω cm^2)	R_p (Ω cm^2)	R_T (Ω cm^2)
NR211	H_2/Air Pambient	0.14	0.72	0.86
	H_2/Air +1bar	0.10	0.57	0.67
	H_2/Air +2bar	0.16	0.52	0.68
	H_2/O_2 Pambien	0.13	0.35	0.47
	H_2/O_2 Air +1bar	0.11	0.31	0.43
	H_2/O_2 Air +2bar	0.17	0.32	0.49
XL	H_2/Air Pambient	0.18	0.89	1.06
	H_2/Air +1bar	0.16	0.65	0.80
	H_2/Air +2bar	0.14	0.59	0.73
	H_2/O_2 Pambien	0.18	0.38	0.56
	H_2/O_2 Air +1bar	0.14	0.36	0.50
	H_2/O_2 Air +2bar	0.15	0.35	0.49
NR212	H_2/Air Pambient	0.18	1.25	1.42
	H_2/Air +1bar	0.20	0.76	0.96
	H_2/Air +2bar	0.20	0.60	0.80
	H_2/O_2 Pambien	0.25	0.49	0.73
	H_2/O_2 Air +1bar	0.23	0.37	0.60
	H_2/O_2 Air +2bar	-	-	-
N115	H_2/Air Pambient	0.23	0.70	0.93
	H_2/Air +1bar	0.26	0.62	0.88
	H_2/Air +2bar	0.22	0.76	0.98
	H_2/O_2 Pambien	0.32	0.35	0.68
	H_2/O_2 Air +1bar	0.27	0.43	0.69
	H_2/O_2 Air +2bar	0.37	0.35	0.72

Peak frequency of the depressed semicircles was determined according to the following equation:

$$F_{MAX} = \frac{(R \times Q)^{-\frac{1}{n}}}{2\pi} \quad (2)$$

where *R* represents resistance of the depressed arc, while *Q* and *n* denote pseudo-capacitance and CPE, respectively. Exponent *n* characterizes the phase shift, influencing the positioning of the semicircle's centre, which is shifted by (1-n*) x 90°* below Z_{Real} axis. Then, total resistance was calculated as:

$$R_T = R_\Omega + R_P \quad (3)$$

As shown in Table 2, increasing operating pressure generally leads to a decrease in R_P, while the use of pure oxygen instead of air significantly reduces R_P, leading to lower R_T values and highlighting the impact of oxygen availability on performance. Among the tested membranes, NR211 exhibited the lowest R_Ω, particularity under pressurized conditions, whereas N115 showed the highest overall resistance. These results confirm that both operating and membrane thickness strongly influence the electrochemical behaviour and resistance distribution of the MEAs.

Scanning Electron Microscopy (SEM)

Cross-sectional analysis of MEAs was conducted using backscattered electron mode to enhance the visibility of the catalytic layer (Fig. 7). Nafion® N115, the thickest membrane, at approxim. 125 µm, showed a substantial bulk increase in its SEM cross-section. This additional thickness contributes to increased internal resistance and obstructs gas diffusion, thereby lowering overall efficiency and power output of the fuel cell.

Results show that Nafion®'s ionomer content does not significantly affect the thickness of the catalytic layer. SEM images provide detailed insights into structural variations among MEAs utilizing Nafion® membranes NR211, XL, NR212, and N115, crucial for understanding how membrane thickness influences PEM fuel cell performance.

Nafion® NR21 displayed a compact and uniform morphology, with its low thickness contributing to reduce R_Ω and improve proton conductivity, which explain its superior electrochemical performance, and making it ideal for high-efficiency applications. Nafion® XL, although no longer commercially available, exhibited an intermediate thickness with a mechanically reinforced structure, resulting in a balanced design compared to NR211. Nafion® NR212, demonstrated a visibly more robust structure than NR211; this increases thickness leads to higher internal resistance and potentially lower which could negatively affect overall MEA's performance.

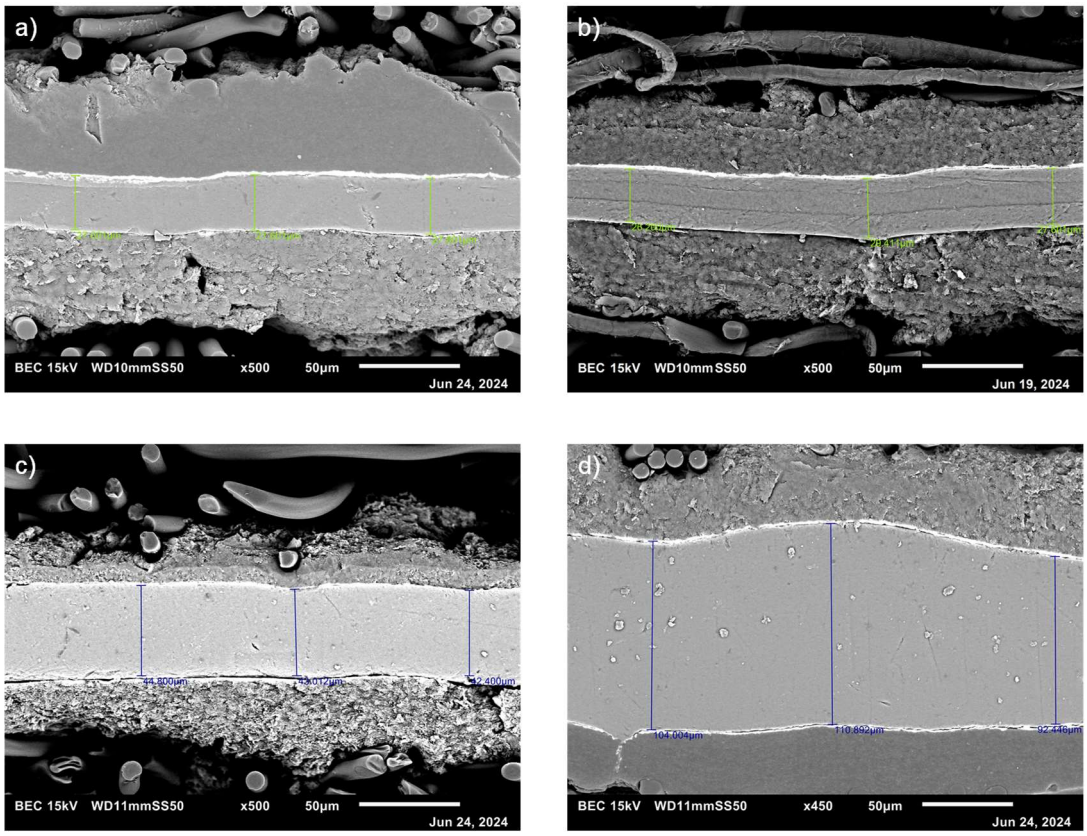

Figure 7: Cross-sectional images of the MEAs with various Nafion® membranes are shown, highlighting structural differences: **(a)** NR211, **(b)** XL, **(c)** NR212, and (**d)** N115.

Comparative study of the effect of reducing Pt loading

As discussed previously, Nafion® NR211 and XL membranes demonstrated superior performance in PEM fuel cell tests. However, since Nafion® XL is no longer commercially available, subsequent experiments will focus on NR211 and NR212, the latter being the third-best performing Nafion® membrane in earlier evaluations. At this stage, the focus shifted toward reducing platinum loading in catalytic ink to investigate its impact on electrochemical performance, particularly regarding cost-efficiency and catalyst utilization.

MEAs analysed in this section were fabricated using a fixed amount of catalyst (40% Pt/C, HISPEC 4000) but, in this case, incorporated Nafion® NR211 and NR212 membranes. Catalytic layers were prepared with the same platinum loadings as in previous experiments, maintaining a total loading of 0.15 mg_{Pt} cm^{-2} across the entire cell. In addition, following the experimental procedure describe in the Materials and Methods section, all MEAs were characterized using the same established protocol, accordingly, this section focuses exclusively on the results obtained after applying this methodology.

First, prior to electrochemical characterization, the MEAs were subjected to a 20 h electrical conditioning step in single-cell configuration at a constant current density of 200 mA cm^{-2}. The evolution of the voltage during this activation period is shown in Fig. 8, where all cells exhibited transient voltages behaviour until reaching a steady-state response.

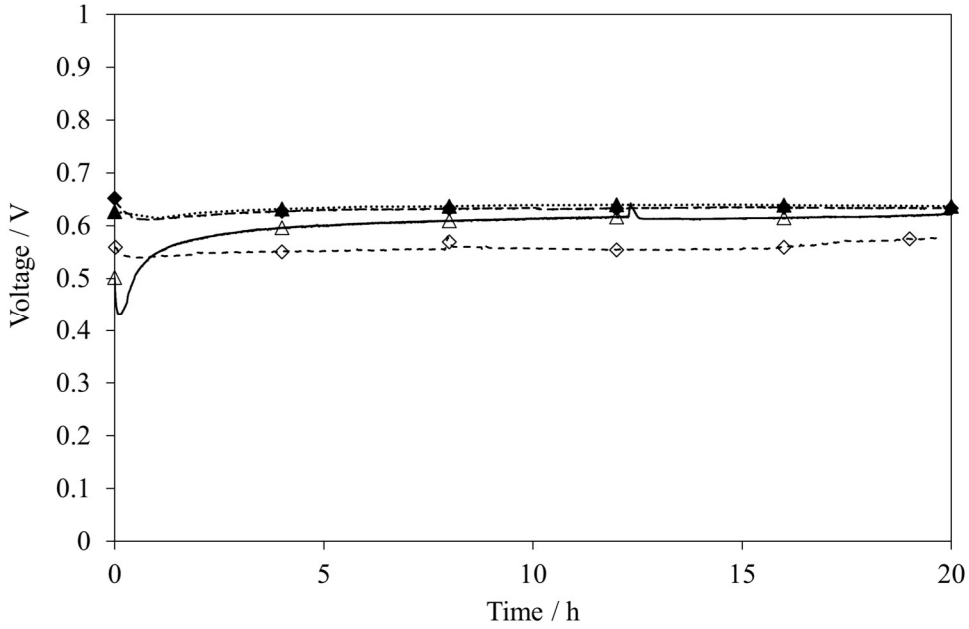

Figure 8: Voltage-time curves of MEAs tested at a current density of 0.2 A cm^{-2}, with H_2/air supplied at atm pressure during 20 ~~hrs~~. The symbols represent different platinum loadings and Nafion® membranes- △ NR211; ◇ NR212; 60% and 40% Pt/C (full symbols).

In this context, the voltage-time profiles reveal differences in stability among the tested MEAs. In general, NR211-based MEAs showed more stable operation and higher steady-state voltages NR212-based systems, consistent with the lower internal resistant associated with the thinner membrane.

Regarding catalyst loading, lower Pt content (40% Pt/C) led to comparable or even improved performance compared to 60% Pt/C, indicating that increasing Pt loading does not necessarily imply a better utilization of Pt or higher cell voltages. This suggest that optimized catalyst utilization can be achieved at reduced Pt content, particularly in MEAs based on NR211.

Subsequently, after the activation step, electrochemical performance was evaluated through polarization curves and electrochemical impedance spectroscopy. Data obtained from the electrochemical analysis technic are summarized in Table 3 and measurements performed following the same test protocol of the previous section are detailed in Fig. 9.

Table 3: OCV, P_{max}, and Pt_{TC} at P_{max} for the tested MEAs at 40% Pt/C under different gas compositions and operating pressures.

Naflon®	**OCV (V)** **Pmax (mW cm^{-2})** **Pt_{TC} (g_{Pt} kW^{-1})**	**H_2/Air** **Pambient**	**H_2/Air** **+1bar**	**H_2/Air** **+2bar**	**H_2/O_2** **Pambient**	**H_2/O_2** **+1bar**	**H_2/O_2** **+2bar**
NR211	OCV	0.816	0.851	0.876	0.849	0.885	0.903
	Pmax	207	293	333	386	498	560
	Pt_{TC}	0.067	0.051	0.047	0.036	0.028	0.025
NR212	OCV	0.923	0.923	0.933	0.908	0.936	0.951
	Pmax	214	312	353	448	601	686
	Pt_{TC}	0.066	0.049	0.046	0.031	0.024	0.020

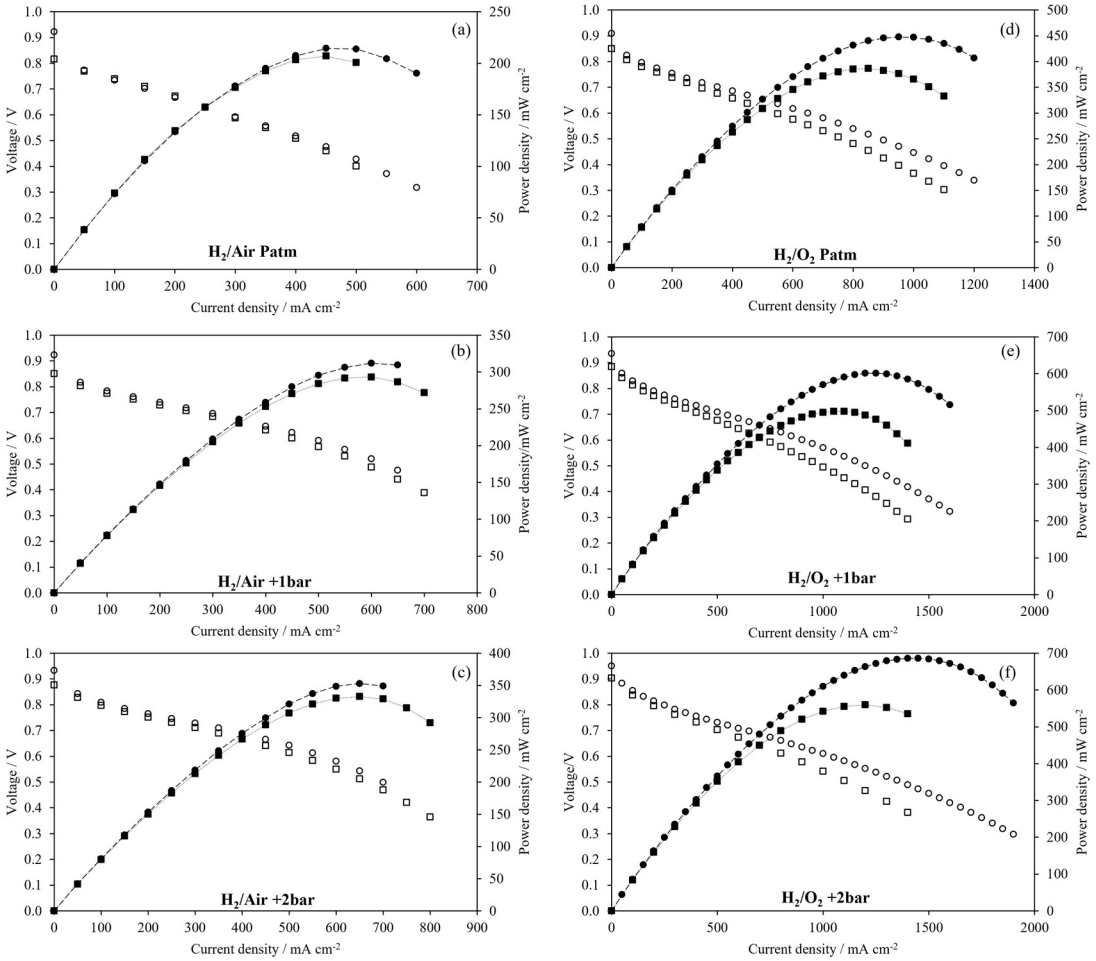

Figure 9: Current density-voltage (I-V) and current density-power density (I-P) curves of MEAs. The symbols represent different platinum loadings and Nafion® membranes:- ☐ 40% Pt/C with NR211; ○ 40% Pt/C with NR212. Measurements were conducted using H_2/air (**a, b, c**) and H_2/O_2 (**d, e, f**) as reactant gases under varying pressures: back pressure **(a, d)**, +1 bar back pressure **(b, e)** and +2 bar back pressure *(c, f)*.

Under these conditions, increasing backpressure from atmospheric conditions to +1bar and +2bar enhanced cell performance, mainly reducing by improving reactant transport and reducing mass transport limitations, with a secondary effect on ohmic resistance.

Similarly, replacing air with pure oxygen significantly improved performance, highlighting the role of oxygen availability in reaction kinetics.

Consistently, polarization curves show that maximum power density increases with both operating pressure and oxygen concentration for all MEAs. These trends are further illustrated in Fig. 10, which compares the power density enhancement across the different Nafion® membranes.

Among the tested configurations, NR212 generally exhibited the highest power output under the most operating conditions.

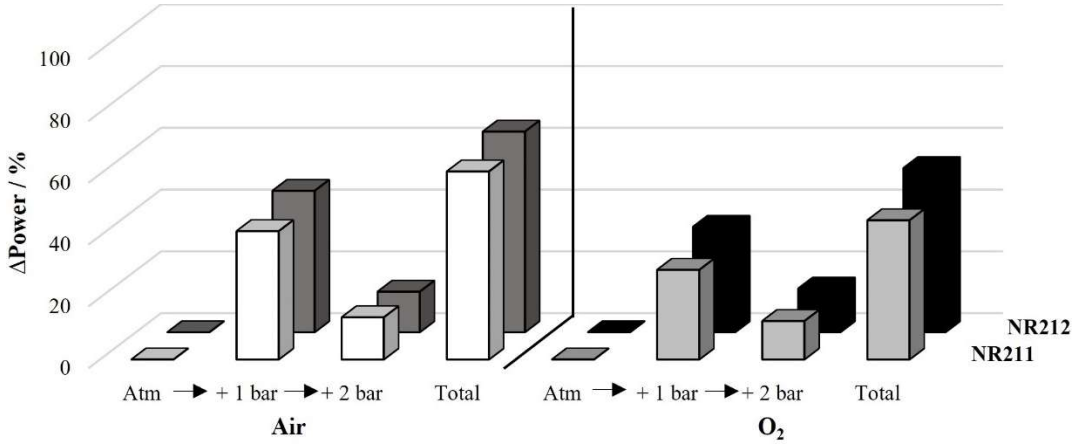

Figure 10: Pmax variations as a function of the two Nafion® membranes studied with the different operation conditions tested.

Moreover, these findings are in agreement with the data obtained from EIS shown in Fig. 11 and Table 4, where Nyquist diagrams highlight differences in charge transfer and mass transport resistances among the two membranes.

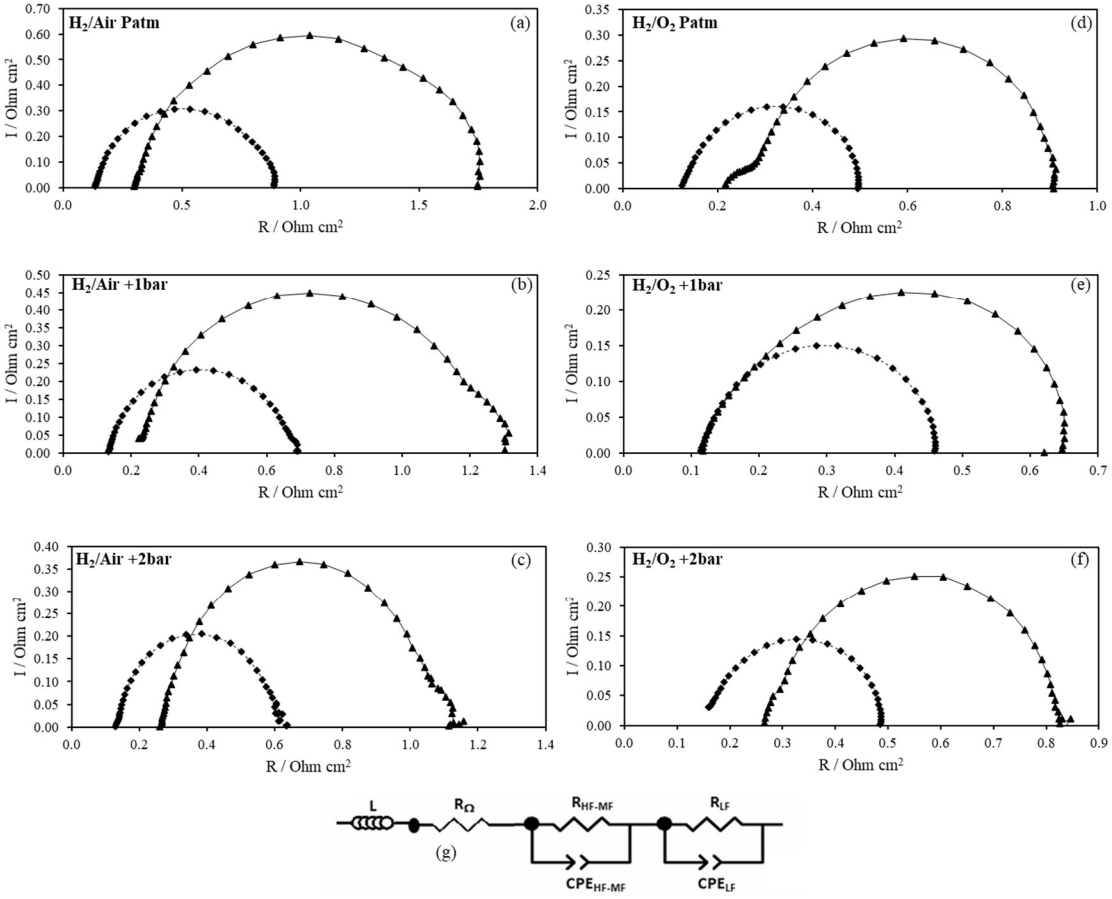

Figure 11: Nyquist diagrams (**a-f**) for MEAs incorporating different Nafion® membranes: △ NR211 and ◇ NR212, tested under galvanostatic mode (1 A) across a frequency range of 0.1 Hz to 100 kHz under various gas compositions and operating pressures. Additionally, (**g**) shows the corresponding equivalent circuit used for fitting the impedance data.

Table 4: Estimated ohmic resistance, polarization resistance and total resistance of the studied MEAs under different gas and pressure operation modes.

Naflon®	Gas mode pressure	RΩ (Ω cm^2)	R_P (Ω cm^2)	R_T (Ω cm^2)
	H_2/Air Pambient	0.30	1.45	1.75
	H_2/Air +1bar	0.23	1.08	1.30
	H_2/Air +2bar	0.26	0.88	1.14
	H_2/O_2 Pambient	0.22	0.69	0.91
	H_2/O_2 Air +1bar	0.12	0.53	0.65
	H_2/O_2 Air +2bar	0.26	0.58	0.85
	H_2/Air Pambient	0.13	0.75	0.89
	H_2/Air +1bar	0.13	0.55	0.69
	H_2/Air +2bar	0.13	0.51	0.64
	H_2/O_2 Pambient	0.12	0.37	0.49
	H_2/O_2 Air +1bar	0.11	0.35	0.46
	H_2/O_2 Air +2bar	0.18	0.30	0.49

In summary, as previously discussed, operating conditions (oxidant type and pressure) and membrane properties play a key role in determining PEMFC performance. In addition to these factors, the present results indicate that the platinum loading in the catalyst layer does not significantly improve the overall performance of the MEAs. In fact, in some cases a lower Pt content leads to a comparable or even slightly enhanced performance, suggesting more efficient catalyst utilization under these conditions. Therefore, the combined effect of membrane characteristic and operating parameters remains the dominant factor governing MEA behaviour, while catalyst loading appears to have a secondary or non-linear influence within the range investigated.

Furthermore, the dataset obtained from this work could be very useful as a reference for further comparisons with MEAs of different catalyst loadings, providing insight into the role of platinum content in optimizing fuel cell efficiency.

Conclusions

From this work, the following conclusions can be drawn:

-A robust testing protocol for PEMFC has been developed, comprising three key steps: activation, polarization curve measurements (current-voltage), and EIS. The polarization and impedance tests were repeated to evaluate the effects of the oxidant (air or oxygen) and operating pressure, with parameters adjusted sequentially: air atmospheric → air + 1 bar → air + 2 bar → O_2 atmospheric → O_2 + 1 bar → O_2 + 2 bar.

-Increasing the operating pressure consistently improved the maximum power density across all four MEAs, regardless of the oxidant used. Switching from air to oxygen resulted in significant power increases of 57.3, 56.6, 54.3, and 37.2% for MEAs incorporating Nafion® NR211, XL, NR212, and N115, respectively.

These findings indicate that, as membrane thickness increases, PEM fuel cell performance declines due to higher internal resistance.
-MEA with Nafion® NR211 (25 μm thickness) achieved the highest performance, clearly demonstrating that reducing the thickness of the fluorinated polymer membrane not only preserves functionality but enhances it. This insight will guide future research efforts, highlighting the importance of optimizing membrane thickness to achieve superior PEM fuel cell performance.
-The reduction of platinum content in the catalyst from 60 to 40% Pt/C for the two membranes studied (NR211 and NR212) revealed that both membranes maintain relatively stable performance trends, confirming their suitability when the Pt concentration in the catalyst is reduced. Furthermore, this new catalyst formulation yielded better results than the previous one, when the PEM fuel cell was operated with H_2/O_2 and under higher back pressures, where the catalytic limitations of lower Pt loading become more evident.
-For future work, it would be of interest to investigate how the reduction of catalytic loading and the influence of the Nafion/catalyst ratio in the formulation of the catalytic ink affect the performance of PEMFC.

Acknowledgements
This research was funded by Complementary Renewable Energy and Hydrogen Plan of the Recovery, Transformation and Resilience Plan funded by the European Union-Next Generation-EU, grant number C17.I01.P01 & State Research Agency, Ministry of Science, Innovation and Universities (Spain), grant number PID2020 115935RA C44.

Declaration of competing interest
The authors declare that they have no known competing financial interests or personal relationships that could influence the work reported in this paper.

Authors' contributions
Julia Isidro: investigation; validation; formal analysis; writing – review and editing. **Lidia Sánchez-Beato**: investigation; writing – original draft; methodology; data curation. **Irene Ayuso**: investigation; writing – original draft; methodology; data curation. **Jesús Rodríguez**: conceptualization; validation; formal analysis; writing – review and editing. **Roberto Campana**: conceptualization; funding acquisition; supervision; writing – review and editing.

Abbreviations
CPE: Constant-Phase Element
EIS: Electrochemical Impedance Spectroscopy
MEAs: Membrane Electrode Assemblies
OCV: Open-Circuit Voltage

PEMFCs: Proton Exchange Membrane Fuel Cells
P_{max}: maximum power densities
Pt_{TC}: Pt-specific power parameter
KPIs: Key Performance Indicators
R_{Ω}: ohmic resistance
R_P: polarization resistance
R_T: total resistance
SEM: Scanning Electron Microscopy

References

1. Karlilar S, Pata UK. Comparative analysis of the impacts of solar, wind, biofuels and hydropower on load capacity factor and sustainable development index. Energy. 2025;319. https://doi.org/10.1016/j.energy.2025.134991
2. Nwagu CN, Ujah CO, Kallon DVV et al. Integrating solar and wind energy into the electricity grid for improved power accessibility. Unconv Res. 2025;5:100129. https://doi.org/10.1016/j.uncres.2024.100129
3. Weißensteiner F. Competitiveness of green and yellow Hydrogen: A project-level analysis. J Clean Prod. 2025;496:144998. https://doi.org/10.1016/j.jclepro.2025.144998
4. Kahraman H, Akın Y. Recent studies on proton exchange membrane fuel cell components, review of the literature. Energy Convers Manag. 2024;304:118244. https://doi.org/10.1016/j.enconman.2024.118244
5. Enasel E, Dumitrascu G. Storage solutions for renewable energy: A review. Ener Nex. 2025;17:100391. https://doi.org/10.1016/j.nexus.2025.100391
6. Hafis M, Balaji K, Tamilarasan N et al. A review on alternative fuels: Spray characteristics, engine performance and emissions effect. Sustain Fut. 2025;9:100456. https://doi.org/10.1016/j.sftr.2025.100456
7. Alinejad Z, Parham N, Tawalbeh M et al. Progress in green hydrogen production and innovative materials for fuel cells: A pathway towards sustainable energy solutions, Int J Hydrogen Energy 2024;140:1078-94. https://doi.org/10.1016/j.ijhydene.2024.09.153
8. Mališ J, Mazúr P, Paidar M et al. Nafion 117 stability under conditions of PEM water electrolysis at elevated temperature and pressure. Int J Hydrog Ener. 2016;41:2177-88. https://doi.org/10.1016/j.ijhydene.2015.11.102
9. Reed D, Thomsen E, Wang W et al. Performance of Nafion® N115, Nafion® NR-212, and Nafion® NR-211 in a 1 kW class all vanadium mixed acid redox flow battery. J Pow Sour. 2015;285:425-30. https://doi.org/10.1016/j.jpowsour.2015.03.099
10. Vasu G, Sreenivasulu B, Sarma GVS et al. Effect of Humidifier Temperatures on Nafion-XL Membrane Electrode Assemblies (MEA)-An Experimental Study. Part 1. Mater Tod Proceed. 2018;5(1):765-71. https://doi.org/10.1016/j.matpr.2017.11.145

11. Liu Z, Yang WW, Zhang JR et al. Gradient catalyst layer design for low-Pt-loading PEM fuel cell based on artificial neural network and multi-objective optimization, Int J Hydrog Ener. 2025;141:650-64. https://doi.org/10.1016/j.ijhydene.2024.12.520
12. De Oliveira PN, Mendes AMM. Preparation and characterization of an eco-friendly polymer electrolyte membrane (PEM) Based in a Blend of Sulphonated Poly(Vinyl Alcohol)/Chitosan Mechanically Stabilised by Nylon 6,6. Mater Res. 2016;19:954-62. https://doi.org/10.1590/1980-5373-MR-2016-0387
13. Xing L, Wang Y, Das PK et al. Homogenization of current density of PEM fuel cells by in-plane graded distributions of platinum loading and GDL porosity. Chem Eng Sci. 2018;192:699-713. https://doi.org/10.1016/j.ces.2018.08.029
14. Zeis R, Mathur A, Fritz G et al. Platinum-plated nanoporous gold: An efficient, low Pt loading electrocatalyst for PEM fuel cells. J Pow Sour. 2007;165:65-72. https://doi.org/10.1016/j.jpowsour.2006.12.007
15. González LR, Campana MP, Sanchez-Molina M et al. Study of the influence of Nafion/C composition on electrochemical performance of PEM single cells with ultra-low platinum load. Int J Hydrogen Energy. 2021;46:17550-61. https://doi.org/10.1016/j.ijhydene.2020.03.114
16. Weber AZ, Borup RL, Darling RM et al. A Critical Review of Modeling Transport Phenomena in Polymer-Electrolyte Fuel Cells. J Electrochem Soc. 2014;161:F1254. https://doi.org/10.1149/2.0751412jes
17. Huang J, Li Z, Zhang J. Review of characterization and modeling of polymer electrolyte fuel cell catalyst layer: The blessing and curse of ionomer. Front Ener. 2017;11:334-64. https://doi.org/10.1007/s11708-017-0490-6
18. Zhang J, Song C, Zhang J et al. Understanding the effects of backpressure on PEM fuel cell reactions and performance. J Electroanalyt Chem. 2013;688:130-36. https://doi.org/https://doi.org/10.1016/j.jelechem.2012.09.033
19. Tsotridis G, Pilenga A, De Marco G et al. EU Harmonised Test Protocols for Pemfc Mea Testing in Single Cell Configuration for Automotive Applications. 2015. https://doi.org/10.2790/54653
20. Kusoglu A, Weber AZ. New Insights into Perfluorinated Sulfonic-Acid Ionomers. Chem Rev. 2017;117:987-1104. https://doi.org/10.1021/acs.chemrev.6b00159
21. Yan X, Xu Z, Yuan S et al. Structural and transport properties of ultrathin perfluorosulfonic acid ionomer film in proton exchange membrane fuel cell catalyst layer: A review. J Pow Sour. 2022;536: 231523. https://doi.org/10.1016/j.jpowsour.2022.231523
22. Tang Z, Huang QA, Wang YJ et al. Recent progress in the use of electrochemical impedance spectroscopy for the measurement, monitoring, diagnosis and optimization of proton exchange membrane fuel cell performance. J Pow Sour. 2020;468:228361. https://doi.org/10.1016/j.jpowsour.2020.228361